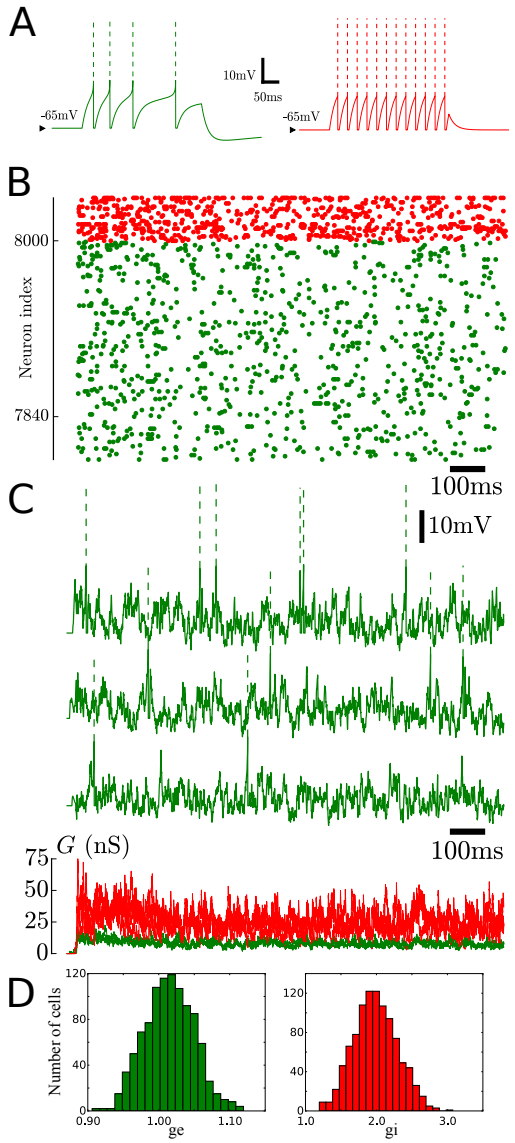

FIG. 2. **Biophysically realistic network model of AI states**. (color online) A. Two cell types used in the model, respectively for excitatory (RS cell, green) and inhibitory (FS cell, red). The traces show typical responses to depolarizing current pulses. B. Raster of activity during an AI state generated by this network. C. Examples of excitatory cells (top, green traces) and their total synaptic conductance (red inhibitory, green excitatory). D. Conductance distribution in this network, normalized to the leak conductance. Parameters are given in Appendix.

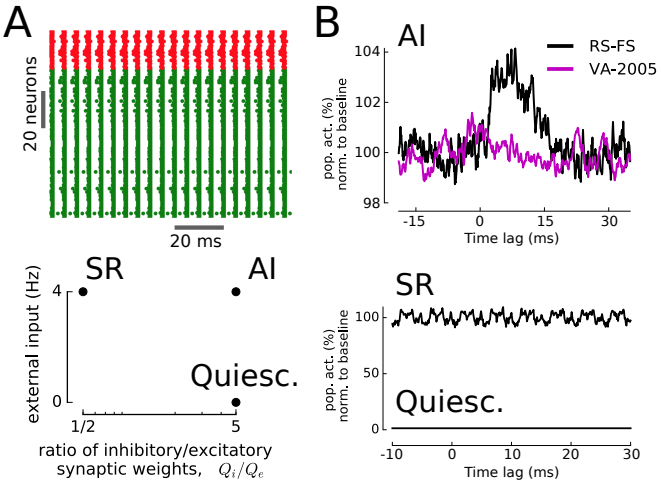

FIG. 3. **Enhanced responsiveness in AI states at the network level**. (color online) A. Three different states in the parameter space of the RS-FS cells network, synchronous regular (SR), asynchronous irregular (AI) and quiescent (Quiesc). B. Responsiveness of the network according to its activity state. The average population response is shown for an excitatory input randomly distributed on a subset of cells (1 single EPSP of 1nS distributed in 40 cells; average of 4000 trials). The response in another network [5] (VA-2005), with aberrant conductance state, is shown for comparison (magenta).

However, in a network displaying an aberrant conductance state, this response was not present. The response was also absent in a quiescent state, or in an oscillatory state in the same network (Fig. 3B). This shows that the AI state, if with correct conductance and V_m fluctuations, displays an enhanced responsiveness to external inputs, and is able to collectively detect inputs of very small amplitude, which normally would have been subthreshold.

We have done additional simulations to explore how responsiveness depends on conductance state, by considering random sets of parameters around the AI state in Fig. 3A. This exploration showed that the responsiveness highly depends on the conductance state of the network (Fig. 4). The response was quantified as the area of the evoked population response (as in Fig. 3B), represented against the total conductance, as calculated from distributions (as in Fig. 2D). One can see that the response is indeed high for physiological conductance states (gray area in Fig. 4) and approaches to zero for aberrant conductance states. This result explains the difference of responsiveness between the two networks shown in Fig. 3B (top). However, it is important to keep in mind that the response also depends on the level of fluctuations and the average V_m level, which can be quantified by considering distributions of the standard deviation of the membrane potential (σ_V) and of the mean V_m of the cells (not shown). The responsiveness can also be understood using a phenomenological model, as shown recently [24].

This phenomenon of network-level responsiveness is very similar to the enhanced responsiveness that was found earlier at the single neuron level [23]. In single-cell studies, the presence of synaptic "noise" conferred an anhanced sensitivity to the neuron. It was also shown that having the correct conductance state and fluctuation regime of the cell is important, it sets the response to a realistic level, and enhanced responsiveness was present using the conductances measured experimentally, as well as their level of fluctuations. Enhanced responsiveness was also found in noisy networks, either in feedforward networks where all cells display a high-conductance state [23], or in chaotic recurrent networks where the enhanced responsiveness was quantified in terms of information transport [25, 26]. One of these studies was the first to demonstrate that networks in a chaotic state display enhanced responsiveness [25]. We complement here these previous studies by showing that

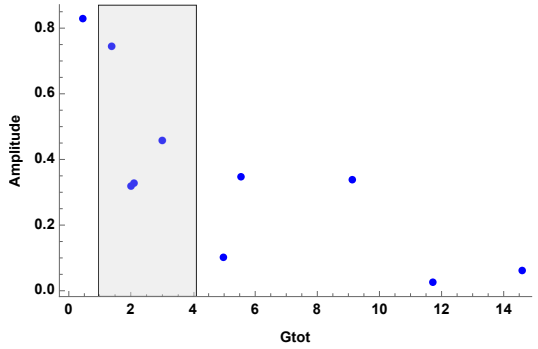

FIG. 4. **Ehanced responsiveness depends on conductance state.** (color online) The average response is represented against the total conductance, for randomly selected parameter sets displaying AI states. The response was computed as the integral of the population response (as in Fig. 3B), above the baseline. The total conductance was calculated as the sum of the average conductance distributions (as in Fig. 2D), and thus was normalized to the leak conductance. The gray area indicates the conductance range corresponding to physiological measurements in awake animals.

enhanced responsiveness is present in recurrent networks displayin AI states, which are presumably chaotic [2]. In addition, we show that this property highly depends on conductance state, and that physiologically plausible conductance state are particularly responsive. This underlies the importance to work with conductance-based models, as current-based models are unlikely to display the correct responsiveness, and cannot be checked against conductance measurements, so are also unconstrained.

Thus, the present results suggest that the conductance state of a network is a fundamental property to understand its responsiveness, which emphasize the importance of conductance measurements *in vivo*. We suggest that HC states have a universal aspect, in the sense that the conductance and fluctuation level measured *in vivo* are the fundamental parameters that neural networks should reproduce, to yield responsiveness properties relevant to neural function.

Finally, let us emphasize that in the AI state, the network responds instantaneously to an input, and this input can occur at any time, which presents evident useful computational properties. A particularly interesting property is that, when submitted to successive presentations of the same stimulus, different neurons respond on each trial, showing that it is the whole network that is globally "aware" of this stimulus. We therefore propose that such network-level responsiveness during AI states implements a low-level form of sensory awareness in networks of neurons. The fact that this occurs in AI states is consistent with the observation that cerebral cortex is in a "desynchronized" state in awake and attentive states (reviewed in [27, 28]). A recent review concluded that desynchonized cortical activity is so far the best correlate of conscious states [29], but no mechanism was given. We propose here such a possible mechanism to link these high-level aspects to elementary biophysical properties of neurons.

Acknowledgments: Research funded by the CNRS and the European Community (*Human Brain Project* H2020-720270). We thank Yann Zerlaut for many discussions and help with the simulations.

[1] van Vreeswijk C, Sompolinsky H (1996) Chaos in neuronal networks with balanced excitatory and inhibitory activity. *Science* **274**: 1724-1726.
[2] van Vreeswijk, C., & Sompolinsky, H. (1998). Chaotic balanced state in a model of cortical circuits. *Neural Comput.* **10**: 1321-1371.
[3] Amit, D.J. and Brunel, N. (1997) Model of global spontaneous activity and local structured activity during delay periods in the cerebral cortex. *Cerebral cortex* **7**: 237-252.
[4] Brunel, N. (2000) Dynamics of sparsely connected networks of excitatory and inhibitory spiking neurons. *J. Computational Neurosci.* **8**: 183-208.
[5] Vogels, T.P., and Abbott, L.F. (2005) Signal propagation and logic gating in networks of integrate-and-fire neurons. *J. Neurosci.* **25**: 10786-10795.
[6] Destexhe, A. (2009) Self-sustained asynchronous irregular states and updown states in thalamic, cortical and thalamocortical networks of nonlinear integrate-and-fire neurons. *J. Computational Neurosci.* **27**: 493-506.
[7] Yger, P., El Boustani, S., Destexhe, A. and Fregnac, Y. (2011) Topologically invariant macroscopic statistics in balanced networks of conductance-based integrate-and-fire neurons. *J. Computational Neurosci.* **31**: 229-245.
[8] Paré, D., Shink, E., Gaudreau, H., Destexhe, A. and Lang, E.J. (1998) Impact of spontaneous synaptic activity on the resting properties of cat neocortical neurons *in vivo*. *J. Neurophysiol.* **79**: 1450-1460.
[9] Destexhe A and Paré D. (1999) Impact of network activity on the integrative properties of neocortical pyramidal neurons in vivo. *J. Neurophysiol.* **81**: 1531-1547.
[10] Destexhe, A., Rudolph, M. and Paré, D. (2003) The high-conductance state of neocortical neurons in vivo. *Nature Reviews Neurosci.* **4**: 739-751.
[11] Steriade, M., Timofeev, I., and Grenier, F. (2001) Natural waking and sleep states: a view from inside neocortical neurons. *J. Neurophysiol.* **85**: 1969-1985.
[12] Crochet, S., and Petersen, C.C. (2006) Correlating whisker behavior with membrane potential in barrel cortex of awake mice. *Nature neurosci.* **9**: 608-610.
[13] Rudolph, M., Pospischil, M., Timofeev, I. and Destexhe, A. (2007) Inhibition determines membrane potential dynamics and controls action potential generation in awake and sleeping cat cortex. *J. Neurosci.* **27**: 5280-5290.
[14] Destexhe, A., Rudolph, M., Fellous, J. M. and Sejnowski, T. J. (2001) Fluctuating synaptic conductances recreate in vivo-like activity in neocortical neurons. *Neuroscience* **107**: 13-24.
[15] Chance, F. S., Abbott, L. F and Reyes, A. D. (2002) Gain modulation from background synaptic input. *Neuron* **35**: 773-782.
[16] Rauch, A., La Camera, G., Luscher, H. R., Senn, W. and Fusi, S. (2003) Neocortical pyramidal cells respond as integrate-and-fire neurons to in vivo-like input currents. *J. Neurophysiol.* **90**: 1598-1612.
[17] Wolfart, J., Debay, D., Le Masson, G., Destexhe, A. and Bal, T. (2005) Synaptic background activity controls spike transfer from thalamus to cortex. *Nature Neurosci.* **8**: 1760-1767.
[18] Prescott, S. A., Ratté, S., De Koninck, Y., and Sejnowski, T. J. (2008) Pyramidal neurons switch from integrators in vitro to resonators under in vivo-like conditions. *J. Neurophysiol.* **100**: 3030-3042.

[19] Zerlaut, Y., Telenczuk, B., Deleuze, C., Bal, T., Ouanounou, G. and Destexhe, A. (2016) Heterogeneous firing rate response of mice layer V pyramidal neurons in the fluctuation-driven regime. *J. Physiol.* **594**: 3791-3808.

[20] El Boustani, S., Pospischil, M., Rudolph-Lilith, M. and Destexhe, A. (2007) Activated cortical states: experiments, analyses and models. *J. Physiol. Paris* **101**: 99-109.

[21] McCormick, D.A., Connors, B.W., Lighthall, J.W. and Prince, D.A. (1985) Comparative electrophysiology of pyramidal and sparsely spiny stellate neurons of the neocortex. *J. Neurophysiol.* **54**: 782-806.

[22] Brette, R. and Gerstner, W. (2005) Adaptive exponential integrate-and-fire model as an effective description of neuronal activity *J. Neurophysiol.* **94**: 3637-3642.

[23] Hô, N. and Destexhe, A. (2000) Synaptic background activity enhances the responsiveness of neocortical pyramidal neurons. *J. Neurophysiol.* **84**: 1488-1496.

[24] Reig, R., Zerlaut, Y., Vergara, R., Destexhe, A. and Sanchez-Vives, M. (2015) Gain modulation of synaptic inputs by network state in auditory cortex in vivo. *J. Neurosci.* **35**: 2689-2702.

[25] Destexhe, A. (1994) Oscillations, complex spatiotemporal behavior and information transport in networks of excitatory and inhibitory neurons. *Physical Review E* **50**: 1594-1606.

[26] Destexhe, A. and Contreras, D. (2006) Neuronal computations with stochastic network states. *Science* **314:** 85-90.

[27] Niedermeyer, E., and da Silva, F. L. (Eds.). (2005) *Electroencephalography: basic principles, clinical applications, and related fields.* Lippincott Williams and Wilkins, New York.

[28] Steriade, M. M., and McCarley, R. W. (2013) *Brainstem control of wakefulness and sleep*, Springer, New York.

[29] Koch, C., Massimini, M., Boly, M., and Tononi, G. (2016) Neural correlates of consciousness: progress and problems. *Nature Reviews Neurosci.* **17**: 307-321.

APPENDIX

Details of the network model

The network model used here consisted of excitatory (RS) and inhibitory (FS) neurons described by the Adaptive Exponential integrate and fire model [22], for which the equations for the membrane potential and the adaptation current read:

$$\begin{cases} C_m \dfrac{dV}{dt} = g_L \left(E_L - V\right) + I_{syn}(V,t) + k_a e^{\frac{V-V_{thre}}{k_a}} - I_w \\ \tau_w \dfrac{dI_w}{dt} = -I_w + \displaystyle\sum_{t_s \in \{t_{spike}\}} b\ \delta(t-t_s) \end{cases},$$

where V is the membrane potential, C_m is the membrane capacitance, g_L is the resting conductance and E_L its reversal potential, I_{syn} is the synaptic current, k_a and V_{thre} are threshold parameters. I_w is the adaptation current, which evolved according to a time constant τ_w and increases by a value b at each spike t_s. FS cells correspond to the same model with I_w=0.

The cellular parameters were, for RS cells: g_L=10nS, C_m=200pF, T_{ref}=5ms, E_L=-70mV, V_{thre}=-50mV, V_{reset}=-70mV, k_a=2mV, a=4nS, b=20pA, τ_w=500ms. FS cells were descrivbed by a leaky integrate and fire model with g_L=10nS, C_m=200pF, T_{ref}=5ms, E_L=-70mV, V_{thre}=-50mV, V_{reset}=-70mV. Network parameters: 4000 RS and 1000 FS cells, connectd randomly with probability of 5%, and with synaptic weights of Q_e=1nS and Q_i=5nS (with respective reversal potentials of E_e=0mV, E_i=-80mV). The synaptic conductances were decaying exponentials with a time constant of 5 ms.

An external drive was present in all neurons and consisted of 4000 independent Poisson processes (rate of 4 Hz), projected over the 5000 neurons with 5% connection probability (weight of 1nS).

The external stimulus of Fig 3 consisted of 40 synchronous EPSPs of 1nS, spread over 40 randomly-choosen excitatory neurons within the population.